BUTTERWORTH HEINEMANN

Nonsimilar solutions for mixed convection on a wedge embedded in a porous medium

J. V. C. Vargas,* T. A. Laursen,† and A. Bejan*
Department of Mechanical Engineering and Materials Science* and Civil and Environmental Engineering,†
Duke University, Durham, NC, USA

The problem of mixed convection on a wedge in a saturated porous medium is analyzed using the Darcy flow formulation and three different methods of solution. Nonsimilar solutions are obtained for several wedge angles. The nonsimilarity technique is applied to the boundary layer formulation, and the finite element method is used in both formulations. It is shown that both formulations produce results that agree well for Pe = 1 and uniform wall temperature in the range $0.1 \leq Ra/Pe \leq 100$. The local and average Nusselt numbers are calculated for several geometries. Relative to the progress documented in the literature, new solutions are presented for $m = 1/3$, 1/2 and 1 (i.e., wedge half angles $\gamma = 45°$, 60°, and 90°). It is shown that the overall heat-transfer rate is the largest when the wedge angle is zero, and the walls are oriented vertically.

Keywords: porous media; mixed convection; nonsimilar solutions

Introduction

The phenomenon investigated in this paper was inspired by such current energy applications as geothermal energy technology and underground disposal of chemical and nuclear waste (Lai et al. 1991). The injection and removal of the geothermal fluids involved in those processes induce pressure gradients that give rise to an imposed external flow. The problem of combined free and forced convection that results has been studied by several authors. Cheng (1977) presented solutions for two particular cases of mixed convection on a wedge in a porous medium (where the problem admits similarity solutions); namely, the vertical isothermal plate and the 90° wedge with constant heat flux. Merkin (1980) used a perturbation method to study the vertical wall with uniform heat flux, where a similarity solution does not exist, and, later, Joshi and Gebhart (1985) presented a solution to the same problem using the method of matched asymptotic expansions. Both approaches relied on boundary-layer approximations, and their validity at low Rayleigh numbers is questionable.

Cheng and Chang (1979), Chang and Cheng (1983), Cheng and Hsu (1984), and Joshi and Gebhart (1984) investigated, for natural convection on a vertical well and on a horizontal surface, the effects of entrainment from the edge of the boundary layer; the axial heat conduction, and the normal pressure gradient, all of them neglected by boundary-layer theory. They used a perturbation series method, finding that for small wall temperature variations, the boundary-layer theory is quite accurate, even at small Rayleigh numbers. The same agreement does not occur for the case of uniform wall heat flux, as was shown by Pop et al. (1989). At the same time, for high Rayleigh numbers, the validity of Darcy's law is questionable, because non-Darcy effects such as inertia become important, as was demonstrated by Poulikakos and Bejan (1985). Also, boundary friction effects have to be considered for high Rayleigh numbers, as was shown by Kim and Vafai (1989) for natural convection about a vertical plate. These points are discussed at length in Nield and Bejan (1992). A review of the research performed on this topic during the last 20 years was presented in Lai et al. (1991).

The objectives of this paper are: (1) to present new solutions for several wedge angles in complete Darcy formulation, which lead to nonsimilarity problems; (2) to verify the accuracy of the boundary-layer formulation results for low Rayleigh numbers, where Darcy's law is considered a good model for the problem; and (3) to determine the geometry where heat transfer is maximum.

Assuming Darcy's law, numerical solutions are obtained with the local nonsimilarity method and a formulation that results from boundary-layer approximations. A Galerkin finite element method is applied both to the boundary layer and to the complete Darcy formulations. In this way, the accuracy of the method of boundary-layer approximations for low Rayleigh numbers is investigated. The local and wall-averaged Nusselt numbers are then computed. Relative to the progress documented in the literature, new solutions are obtained for the wedge with uniform wall temperature and $m = 1/3$, 1/2 and 1 (i.e., $\gamma = 45°$, 60°, and 90°).

Address reprint requests to Professor A. Bejan, Department of Mechanical Engineering, Duke University, Durham, NC 27708-0300, USA.

Received 24 October 1994; accepted 7 March 1995

Int. J. Heat and Fluid Flow 16: 211–216, 1995

655 Avenue of the Americas, New York, NY 10010

0142-727X/95/$10.00
SSDI 0142-727X(95)0024-K

Theoretical model

Figure 1 shows a simple sketch of the problem configuration. The governing equations for convection through a homogeneous porous medium are as follows:

$$\nabla \cdot \mathbf{v} = 0 \tag{1}$$

$$\frac{\mu}{K}\mathbf{v} = -(\nabla p \pm \rho g_i \mathbf{e}_i) \tag{2}$$

$$\mathbf{v} \cdot \nabla T = \nabla \cdot (\alpha \nabla T) \tag{3}$$

The assumptions in deriving Equations 1–3 are that the fluid and the porous medium are in local thermodynamic equilibrium, the fluid temperature is below the boiling point, the fluid properties are homogeneous and isotropic, and the local Reynolds number based on averaged velocity and $K^{1/2}$ does not exceed $O(1)$, which means that Darcy's law is valid. The boundary conditions are as follows:

$$y = 0: \quad v = 0, \quad T_W = \text{constant} \tag{4}$$

$$y \to \infty: \quad u = U_\infty, \quad T = T_\infty \tag{5}$$

The plus sign in Equation 2 accounts for aiding flows and the minus sign for opposing flows.

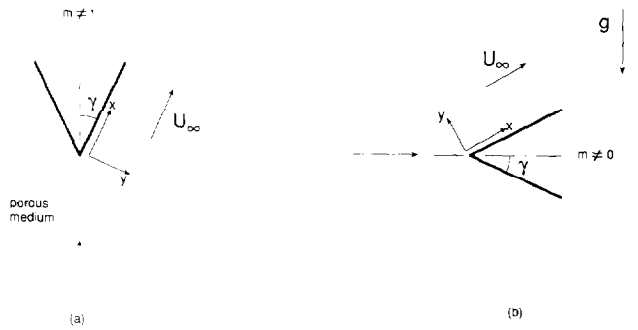

Figure 1 Problem configuration

Formulation with boundary-layer simplifications

A new set of transformed equations is obtained from Equations 1–5 by invoking the Oberbeck–Boussinesq approximation, boundary-layer hypothesis, and by defining the following variables based on scale analysis and the streamfunction Ψ

Notation

A	constant
B	constant
$\mathbf{d}$	solution vector
$\mathbf{e}$	Euclidian unit vector
f	dimensionless function, Equation 7
g	gravitational acceleration, m/s^2
h	dimensionless function, $\partial f/\partial \xi$
H	wall height, m
H^1	functions that satisfy $\int_0^\eta (w')^2 d\eta < \infty$
IN	element integrals of the shape functions, Equations 29–31
k	thermal conductivity, W/m·K
K	permeability, m^2
m	wedge angle parameter, $\gamma/(\pi - \gamma)$
M	capacity matrix
n	exponent, Equation 43
n	wall temperature parameter
N	element shape functions
$\overline{\mathrm{Nu}}$	wall-averaged Nusselt number, Equation 24
Nu_x	local Nusselt number, Equation 12
p	pressure, N/m^2
P	dimensionless pressure, Equation 17
Pe	Peclet number, $U_\infty H/\alpha$
Pe_x	local Peclet number, $U_\infty x/\alpha$
q''	heat flux, W/m^2
Q	stiffness matrix
$\mathbf{R}$	residual vector
Ra	Darcy-modified Rayleigh number, $Kg_x\beta H\Delta T/(\alpha\nu)$
Ra_x	Darcy-modified local Rayleigh number, $Kg_x\beta H\Delta T/(\alpha\nu)$
T	temperature, K
T_W	wall temperature, $Bx^n + T_\infty$
U_∞	free-stream velocity, Ax^m
u, v	velocity components, m/s
U, V	dimensionless velocity components
$\mathbf{v}$	velocity vector, m/s
$\mathbf{V}$	dimensionless velocity vector
w	weighting function
x, y	Cartesian coordinates, m
X, Y	dimensionless coordinates

Greek

α	effective thermal diffusivity of the porous medium, m^2/s
β	coefficient of volumetric thermal expansion, K^{-1}
Γ	dimensionless function, Equation 33
γ	half of the wedge angle
$\Delta\mathbf{d}$	Newton correction for the solution vector
$\Delta\eta$	similarity variable step
$\Delta\xi$	nonsimilarity variable step
ζ	element natural coordinate, $-1 \le \zeta \le 1$
η	similarity variable, Equation 6
θ	dimensionless temperature, Equation 7
μ	viscosity, kg/m·s
ν	kinematic viscosity, m^2/s
ξ	nonsimilarity variable, Equation 6
ρ	density, kg/m^3
ϕ	dimensionless function, $\partial\theta/\partial\xi$
Ψ	dimensionless function, Equation 7
v	weighting space

Superscripts

$(\ )^{(k)}$	Newton iteration
$(\ )^{(j)}$	time-like increment
$(\ )'$	derivatives with respect to η

Subscripts

$(\ )_\infty$	fluid reservoir
$(\ )_i$	Cartesian components, $1 \le i \le 2$
$(\ )_a$	element node, $1 \le a \le 3$

definition $u = \partial\Psi/\partial y$ and $v = -\partial\Psi/\partial x$ (Bejan, 1984):

$$\eta = \frac{y}{x}\,\mathrm{Pe}_x^{1/2}; \qquad \xi = \frac{\mathrm{Ra}}{\mathrm{Pe}_x} \tag{6}$$

$$\Psi = (U_r x\alpha)^{1/2} f(\xi, \eta); \qquad \theta(\xi, \eta) = \frac{T - T_r}{T_w - T_r} \tag{7}$$

The transformed equations are as follows:

$$f'' = \pm\xi\theta' \tag{8}$$

$$\theta'' - n\theta f' + \frac{1+m}{2} f\theta' = (n-m)\xi\left(f'\frac{\partial\theta}{\partial\xi} - \theta'\frac{\partial f}{\partial\xi}\right) \tag{9}$$

subject to the following transformed boundary conditions

$$\eta = 0: \qquad f = 0; \qquad \theta = 1 \tag{10}$$

$$\eta \to \infty: \qquad f' = 1; \qquad \theta = 0 \tag{11}$$

The local Nusselt number $\mathrm{Nu}_x = q''(x, 0)/k(T_w - T_r)$ is given by the following:

$$\frac{\mathrm{Nu}_x}{\mathrm{Pe}_x^{1/2}} = -\theta'(\xi, 0) \tag{12}$$

The nonsimilarity parameter ξ determines whether the physical phenomenon is one of forced, mixed, or free convection.

Formulation without boundary-layer simplifications

The nondimensionalized version of Equations 1–5 based on the Oberbeck–Boussinesq approximation, but without boundary-layer assumptions is the following:

$$\nabla\cdot\mathbf{V} = 0 \tag{13}$$

$$\frac{\mathrm{Pe}}{\mathrm{Ra}}\mathbf{V} = -\nabla P \pm \theta\frac{g_i}{g_x}\mathbf{e}_i \tag{14}$$

$$\mathrm{Pe}\,\mathbf{V}\cdot\nabla\theta = \nabla^2\theta \tag{15}$$

where we have used the following nondimensional groups:

$$(X, Y) = \frac{(x, y)}{H}, \qquad (U, V) = \frac{(u, v)}{U_r} \tag{16}$$

$$P = \frac{p \pm \rho g_i x_i}{\rho g_x \beta H(T_w - T_r)} \tag{17}$$

The boundary conditions shown in Figure 2, for the configuration shown in Figure 1(a), are as follows:

A:

$$V = 0; \qquad \theta = 1 \tag{18}$$

B:

$$V = 0; \qquad \frac{\partial\theta}{\partial Y} = 0 \tag{19}$$

C:

$$\frac{\partial V}{\partial Y} = \frac{\partial\theta}{\partial Y} = 0 \tag{20}$$

D:

$$U = 1; \qquad \theta = 0 \tag{21}$$

E:

$$\frac{\partial U}{\partial X} = \frac{\partial V}{\partial X} = \frac{\partial\theta}{\partial X} = 0 \tag{22}$$

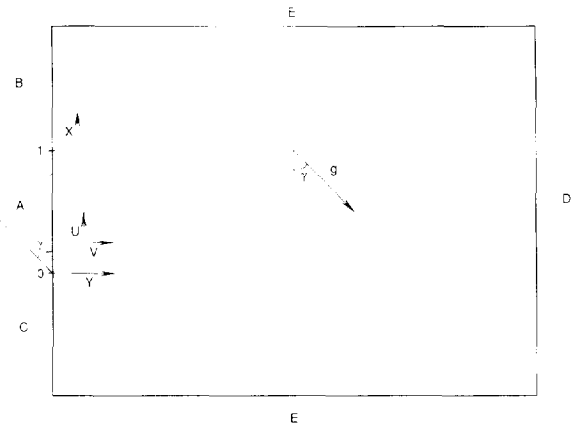

Figure 2 Computational domain for the complete Darcy formulation (without boundary layer assumptions)

The Nusselt number at the downstream end of the wall is the following:

$$\mathrm{Nu}_H = -\left(\frac{\partial\theta}{\partial Y}\right)_{Y=0} \tag{23}$$

It is worth noting that Nu_H can be compared directly with the solution obtained from Equations 8–11, for the case Pe = 1. The wall-averaged Nusselt number $\overline{\mathrm{Nu}}$ is calculated as follows using Equation 12:

$$\frac{\overline{\mathrm{Nu}}}{\mathrm{Pe}_H^{1/2}} = \frac{2}{m+1}\cdot\frac{1}{\xi_{\max}}\int_0^{\xi_{\max}} [-\theta'(\xi, 0)]\,\mathrm{d}\xi \tag{24}$$

Numerical methods and results

The numerical problem consists of solving either Equations 8–11 or Equations 13–22. The equations obtained with boundary-layer approximations were solved by the local nonsimilarity method (Chen, 1988) and by the finite element method. The equations without boundary-layer approximations were solved by the finite element method.

The second level of truncation local nonsimilarity method was applied to Equations 8–11. The method consisted of differentiating Equations 8–11 with respect to ξ. In the new equations, we set $h = \partial f/\partial\xi$ and $\phi = \partial\theta/\partial\xi$. Neglecting the terms that contain $\partial^2(\ )/\partial\xi^2$, we obtain the following equations:

$$h'' = \pm\theta' \pm \xi\phi' \tag{25}$$

$$\phi'' + \left(\frac{1-m}{2} + n\right)h\theta' + (m-2n)f'\phi - nh'\theta + \frac{1+m}{2}f\phi' = (n-m)\xi(h'\phi - h\phi') \tag{26}$$

and the following boundary conditions:

$$\eta = 0: \qquad h = 0; \qquad \phi = 0 \tag{27}$$

$$\eta \to \infty: \qquad h' = 0; \qquad \phi = 0 \tag{28}$$

The numerical task is reduced to solving the boundary-value problem represented by the ordinary differential Equations 8–11 and 25–28. In the application of the shooting method, convergence was guaranteed in the entire ξ-range ($0 \le \xi \le 100$) by using a search scheme to detect the appropriate initial guesses for $f'(\xi, 0)$, $\theta'(\xi, 0)$, $g'(\xi, 0)$, and $\phi'(\xi, 0)$. This search was necessary because as ξ increases, the formulation based on the scales of forced convection becomes inappropriate for natural

convection, and convergence becomes considerably more difficult.

The fourth-order Runge–Kutta method was used to integrate the equations. The tolerance for convergence was 10^{-6}. The values of $\eta_\infty = 10$ and $\Delta\eta = 0.02$ were determined by trial and error (Chen, 1988), so that the same results were obtained with finer meshes and larger η_∞ domains. The 10^{-6} convergence criterion was applied directly to the boundary conditions for f', g', θ, and ϕ at $\eta = \eta_\infty$. To ensure the convergence to an asymptotic solution, the η_∞ values of θ' and f'' were checked simultaneously according to the same tolerance. Numerical computations were carried out for $m = 0$, 1/3, and 1/2 and 1 for $0 \le \xi \le 100$. The local Nusselt numbers are reported in Figures 3 and 4.

In the application of the semidiscrete finite element method: i.e., we leave ξ continuous to begin with and reduce the system 8–11 to a single equation that we discretize in η. Equation 8 can be integrated twice in η to produce an expression for f, which can then be substituted into Equation 9. Performing this operation, using the boundary conditions $f' = 1$ and $\theta = 0$ at $\eta \to \infty$, we obtained the following:

$$f = \xi \int \theta \, d\eta + \eta + \Gamma(\xi) \tag{29}$$

If we utilize quadratic shape functions (Hughes, 1987) for the discretization:

$$\theta = \sum_a N_a d_a \tag{30}$$

we obtain integrals of the shape functions required by Equation 29 via the following:

$$IN_1 = \left(\frac{1}{6}\zeta^3 - \frac{1}{4}\zeta^2\right)\frac{\Delta\eta}{2} \tag{31}$$

$$IN_2 = \left(\zeta - \frac{\zeta^3}{3}\right)\frac{\Delta\eta}{2} \tag{32}$$

$$IN_3 = \left(\frac{1}{6}\zeta^3 + \frac{1}{4}\zeta^2\right)\frac{\Delta\eta}{2} \tag{33}$$

From $f = 0$, $\theta = 1$ at $\eta = 0$ ($\zeta = -1$) and Equations 31–33 in the first element of the η domain, we obtained the following:

$$\Gamma(\xi) = \xi \frac{\Delta\eta}{2}\left(\frac{5}{12} + \frac{2}{3}d_2 - \frac{1}{12}d_3\right) \tag{34}$$

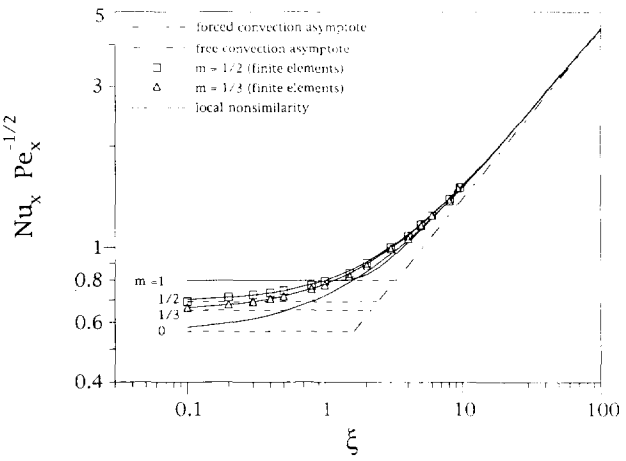

Figure 3 Comparison of results between the local nonsimilarity method and finite elements with boundary-layer approximations

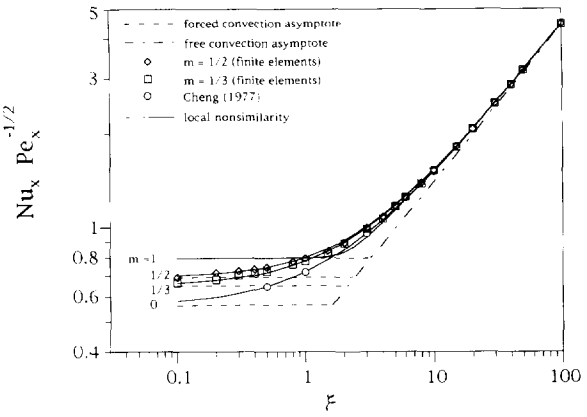

Figure 4 Comparison of results between the local nonsimilarity method and finite elements without boundary-layer approximations (complete formulation)

Next, using the quadratic shape functions and Equations 31–33, we write the following for one element:

$$f = \xi\left(\sum_a IN_a d_a\right) + \sum_a N_a\eta_a + \Gamma(\xi) \tag{35}$$

$$f' = \xi\left(\sum_a N_a d_a\right) + 1 \tag{36}$$

$$\frac{\partial f}{\partial \xi} = \sum_a N_a d_a + \frac{\Delta\eta}{2}\left(\frac{5}{12} + \frac{2}{3}d_2 - \frac{1}{12}d_3\right) \tag{37}$$

Therefore, we numerically treat Equation 9, where we substitute Equations 35–37 for f, f' and $\partial f/\partial\xi$, subject to the temperature boundary conditions. Because this equation is parabolic, the problem is solved implicitly with the backward Euler approach for the time-like discretization; i.e., the discretization in ξ. The initial condition $\theta(0, \eta)$ is obtained directly from the finite elements solution of Equation 9, when $\xi = 0$. The weighting space is defined by the following:

$$\mathcal{V} = \{w | w \in H^1,\ w(0) = w(\eta_\infty) = 0\} \tag{38}$$

The Galerkin discretization is applied after deriving the weak form of the problem. The matrix formulation is expressed schematically as follows:

$$\mathbf{R}^j = Q(\mathbf{d}^j)\cdot\mathbf{d}^j - M(\mathbf{d}^j)\cdot\frac{\mathbf{d}^j - \mathbf{d}^{j-1}}{\Delta\xi} = 0 \tag{39}$$

The Newton–Raphson method is applied in conjunction with a line search scheme to solve the nonlinear system. The last converged solution for the previous value of ξ is used as the predictor for the new ξ solution.

Accuracy tests were performed for several combinations of η_∞, $\Delta\eta$, and $\Delta\xi$. We concluded that $\eta_\infty = 10$; $\Delta\eta = 0.02$; and $\Delta\xi = 0.1$ is the coarsest set, which leads to same results as finer sets. Two convergence criteria were tested for the Newton iteration $|\mathbf{R}|_\infty < 10^{-7}$ and $\Delta\mathbf{d}^{(k)}\cdot\mathbf{R}^{(k)} < 10^{-15}\Delta\mathbf{d}^{(0)}\cdot\mathbf{R}^{(0)}$. Both criteria led to practically identical results.

Numerical results were obtained for $m = 1/2$ and 1/3, which are shown in Figure 3. The procedure diverges after $\xi = 9.6$ for $m = 1/2$, and after $\xi = 9.2$ for $m = 1/3$. The results are in good agreement with the results based on the local nonsimilarity method. The transformed equations were nondimensionalized using the scales of forced convection scale analysis; therefore, convergence became more difficult as ξ increased. To achieve convergence for high values of ξ, Cebeci and Bradshaw (1991) suggested a set of transformed equations based on natural

convection scales. Because after $\xi = O(10)$ natural convection dominates, and the results approach the asymptote known for natural convection, we found it necessary to implement the Cebeci and Bradshaw formulation.

Equations 13–22 were solved using the finite element package FIDAP (1991). The method consisted of Galerkin weighted residuals, and nine nodes isoparametric quadratic elements. Figure 4 shows the results for $m = 1/3$ and $1/2$ (i.e., $\gamma = 45°$ and $60°$), when $\mathrm{Pe} = 1$. These results cover the range $0.1 \leq \mathrm{Ra/Pe} \leq 100$, which, in this, case means $0.1 \leq \mathrm{Ra} \leq 100$. Because our objective was to compute Nu_H for each case, we also used Nu_H to perform accuracy and mesh tests: the results become independent of grid size for 4,941 nodes and 1,200 elements, in the domain drawn to scale in Figure 2.

Figure 4 shows that the results obtained with and without boundary-layer assumptions are in good agreement. These results were obtained for $\mathrm{Pe} = 1$ and $0.1 \leq \mathrm{Ra} \leq 100$ using Darcy's law. Regardless of method, the solution approaches the forced convection asymptote for small ξ and the natural convection asymptote for large ξ. The computational time needed for the solutions based on boundary-layer formulation is much smaller than the time needed for the complete formulation; in conclusion, the agreement between all the solutions indicates that the problem can be solved with economically and reliably by using the boundary-layer formulation. The solution asymptotes are (Cheng, 1977; Bejan, 1984):

$$\frac{\mathrm{Nu}}{\mathrm{Pe}_x^{1/2}} = \theta'(0, 0) \qquad \text{(forced convection)} \tag{40}$$

$$\frac{\mathrm{Nu}_x}{\mathrm{Pe}_x^{1/2}} = 0.444\xi^{1/2} \qquad \text{(natural convection)} \tag{41}$$

The numerical results presented in Figures 3 and 4 are correlated within 5% by an expression of the type recommended by Churchill (1977):

$$\frac{\mathrm{Nu}_x}{\mathrm{Pe}_x^{1/2}} = [(-0.04m^2 + 0.274m + 0.564)^n + 0.444^n \xi^{n/2}]^{1/n} \tag{42}$$

where $0 \leq m \leq 1$, and

$$n = 0.976(1 - m)^3 + 5^m \tag{43}$$

Figure 5 shows the wall-averaged Nusselt number as a function of the wedge half-angle. Results for $m = 1/9$ (or $\gamma = 18°$) were included in Figure 5, so that a smoother curve could be drawn. From the results shown in Figures 3 and 4, we learn that the local Nu value becomes independent of the wedge angle when $\xi = 10$. Therefore, in the calculation of $\overline{\mathrm{Nu}}$ using equation 24 we set $\xi_{\max} = 10$. The wall-averaged Nusselt number has the largest value when $m = 0$; i.e., when the wedge surfaces are oriented vertically.

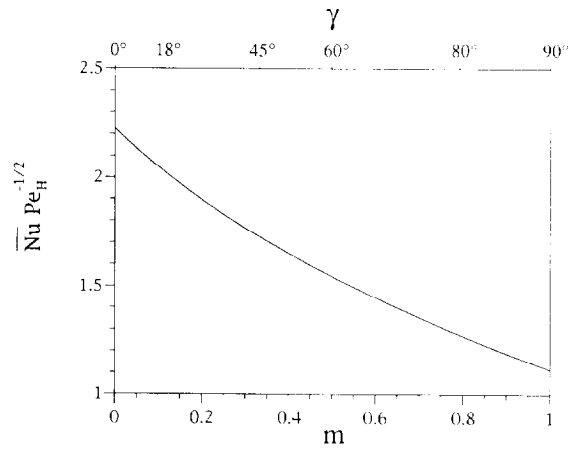

Figure 5 Wall-averaged Nusselt number for $0 \leq m \leq 1$

Conclusions

In this paper, we developed several new heat-transfer solutions for wedge-shaped bodies embedded in a porous medium with forced, mixed, or natural convection. New solutions are obtained for the wedge with uniform surface temperature when $m = 1/3$, $1/2$, and 1 (i.e., $\gamma = 45°$, $60°$, and $90°$). We showed that it is possible to calculate the mixed convection phenomenon in the range of low Ra and low Pe numerically by using a formulation with boundary-layer approximations. We demonstrated this using three numerical methods: (1) local nonsimilarity; (2) finite elements in a boundary-layer formulation; and (3) finite elements in a formulation without boundary-layer approximations. The three sets of results are in very good agreement.

The computational time for solutions with the boundary-layer approximations is much smaller than with the time required by the complete formulation. The agreement between results indicates that the problem can be solved economically using the boundary-layer formulation. In the range $0 \leq m \leq 1$, the overall thermal conductance between the surface and the surrounding medium (or the wall-averaged Nusselt number $\overline{\mathrm{Nu}}$) is the largest when the wedge surface is vertical ($m = 0$).

References

Bejan, A. 1984. *Convection Heat Transfer*, Wiley, New York, Chap. 10

Cebeci, T. and Bradshaw, P. 1991. *Physical and Computational Aspects of Convective Heat Transfer*. Springer-Verlag, New York, Chap. 9

Chang, I. D. and Cheng, P. 1983. Matched asymptotic expansions for free convection about an impermeable horizontal surface in a porous medium. *Int. J. Heat Mass Transfer*, **26**, 163–173

Chen, T. S. 1988. Parabolic systems: local nonsimilarity method. In *Handbook of Numerical Heat Transfer*, W. J. Minkowycz, E. M. Sparrow, G. E. Schneider and R. H. Pletcher (eds.). Wiley, New York, Chap. 5

Cheng, P. 1977. Combined free and forced convection flow about inclined surfaces in porous media. *Int. J. Heat Mass Transfer*, **20**, 807–814

Cheng, P. and Chang, I. D. 1979. Convection in a porous medium as a singular perturbation problem. *Lett. Heat Mass Transfer*, **6**, 253–258

Cheng, P. and Hsu, C. T. 1984. Higher-order approximations for Darcian free convective flow about a semi-infinite vertical flat plate. *J. Heat Transfer*, **106**, 143–151

Churchill, S. W. 1977. A comprehensive correlating equation for laminar, assisting, forced, and free convection. *AIChE J.*, **23**, 10–16

FIDAP Theoretical Manual. 1991. Fluid Dynamics International, Evanston, IL, v. 6.03

Hughes, T. J. R. 1987. *The Finite Element Method*. Prentice-Hall, Englewood Cliffs, NJ, Chap. 3

Joshi, Y. and Gebhart, B. 1984. Vertical natural convection flows in porous media: calculations of improved accuracy. *Int. J. Heat Mass Transfer*, **27**, 169–175

Joshi, Y. and Gebhart, B. 1985. Mixed convection in porous media adjacent to a vertical uniform heat flux surface. *Int. J. Heat Mass Transfer*, **28**, 1783–1786

Kim, S. J. and Vafai, K. 1989. Analysis of natural convection about a vertical plate embedded in a porous medium. *Int. J. Heat Mass Transfer*, **32**, 665–677

Lai, F. C., Kulacki, F. A. and Prasad, V. 1991. Mixed convection in

saturated porous media. In *Convective Heat and Mass Transfer in Porous Media*, S. Kakac, B. Kilkis, F. A. Kulacki and F. Arinc (eds.). Kluwer Academic Publishers, The Netherlands, 225–287

Merkin, J. H. 1980. Mixed convection boundary-layer flow on a vertical surface in a saturated porous medium. *Int. J. Heat Mass Transfer*, **19**, 805–813

Nield, D. A. and Bejan, A. 1992. *Convection in Porous Media*. Springer-Verlag, New York, Chap. 8

Pop, I., Cheng, P. and Le, T. 1989. Leading-edge effects on free convection of a Darcian fluid about a semi-infinite vertical plate with uniform heat flux. *Int. J. Heat Mass Transfer*, **32**, 493–501

Poulikakos, D. and Bejan, A. 1985. The departure from Darcy flow in natural convection in a vertical porous layer. *Phys. Fluids*, **28**, 3477–3483